

Effects of Alkaline Earth Metal Ion Complexation on Amino Acid Zwitterion Stability: Results from Infrared Action Spectroscopy

Matthew F. Bush,[†] Jos Oomens,[‡] Richard J. Saykally,[†] and Evan R. Williams^{*,†}

Department of Chemistry, University of California, Berkeley, California 94720-1460, and FOM Institute for Plasma Physics "Rijnhuizen", Edisonbaan 14, 3439 MN Nieuwegein, The Netherlands

Received December 21, 2007; E-mail: williams@cchem.berkeley.edu

Abstract: The structures of isolated alkaline earth metal cationized amino acids are investigated using infrared multiple photon dissociation (IRMPD) spectroscopy and theory. These results indicate that arginine, glutamine, proline, serine, and valine all adopt zwitterionic structures when complexed with divalent barium. The IRMPD spectra for these ions exhibit bands assigned to carboxylate stretching modes, spectral signatures for zwitterionic amino acids, and lack bands attributable to the carbonyl stretch of a carboxylic acid functional group. Structural and spectral assignments are strengthened through comparisons with absorbance spectra calculated for low-energy structures and the IRMPD spectra of analogous ions containing monovalent alkali metals. Many bands are significantly red-shifted from the corresponding bands for amino acids complexed with monovalent metal ions, owing to increased charge transfer to divalent metal ions. The IRMPD spectra of arginine complexed with divalent strontium and barium are very similar and indicate that arginine adopts a zwitterionic form in both ions. Calculations indicate that nonzwitterionic forms of arginine are lowest in free energy in complexes with smaller alkaline earth metal cations and that zwitterionic forms are preferentially stabilized with increasing metal ion size. B3LYP and MP2 calculations indicate that zwitterionic forms of arginine are lowest in free energy for M = Ca, Sr, and Ba.

Introduction

Isolated amino acids are nonzwitterionic, but complexation with metal ions can preferentially stabilize zwitterionic forms. The structures of amino acids and the effects of metal ion complexation have been widely investigated using a broad range of experimental and computational methods. For example, calculations indicate that the zwitterionic form of isolated proline is not stable,¹ but that this form of proline complexed with monovalent sodium is 12–18 kJ/mol more stable than the nonzwitterionic form.^{2,3} These results are consistent with a variety of experimental studies of the isolated^{4,5} and sodiated^{3,6–9} forms of proline. Larger metal ions can preferentially stabilize the zwitterionic forms of amino acids relative to the nonzwitterionic forms. Both calculations and experiments indicate that

lithiated arginine is nonzwitterionic, but that the zwitterionic form of arginine is preferentially stabilized with increasing alkali metal ion size.^{10–14} Infrared multiple photon dissociation (IRMPD) spectra in both the hydrogen stretch¹³ and fingerprint¹⁴ regions indicate that sodiated arginine is predominately zwitterionic, but that a small population of ions with nonzwitterionic structures is also present. Analogous trends with metal ion size have been reported for alkali metal cationized lysine and ϵ -N-methyllysine,¹⁵ although the opposite trend was reported for sodiated and rubidiated complexes with glycine, alanine, and analogues of these amino acids.¹⁶

Calculations indicate that metal ion charge can also affect the relative stability of the zwitterionic forms of amino acids. For example, the nonzwitterionic form of isolated glycine¹⁷ and alkali metal cationized glycine are lowest in energy, but glycine complexed with all but the smallest alkaline earth metal ion,

[†] University of California, Berkeley.

[‡] FOM Institute for Plasma Physics "Rijnhuizen".

- (1) Lee, K. M.; Park, S. W.; Jeon, I. S.; Lee, B. R.; Ahn, D. S.; Lee, S. *Bull. Korean Chem. Soc.* **2005**, *26*, 909–912.
- (2) Marino, T.; Russo, N.; Toscano, M. *J. Phys. Chem. B* **2003**, *107*, 2588–2594.
- (3) Moision, R. M.; Armentrout, P. B. *J. Phys. Chem. A* **2006**, *110*, 3933–3946.
- (4) Lesarri, A.; Mata, S.; Cocinero, E. J.; Blanco, S.; Lopez, J. C.; Alonso, J. L. *Angew. Chem., Int. Ed.* **2002**, *41*, 4673–4676.
- (5) Stepanian, S. G.; Reva, I. D.; Radchenko, E. D.; Adamowicz, L. *J. Phys. Chem. A* **2001**, *105*, 10664–10672.
- (6) Ye, S. J.; Moision, R. M.; Armentrout, P. B. *Int. J. Mass Spectrom.* **2006**, *253*, 288–304.
- (7) Lemoff, A. S.; Bush, M. F.; Williams, E. R. *J. Phys. Chem. A* **2005**, *109*, 1903–1910.
- (8) Kapota, C.; Lemaire, J.; Maître, P.; Ohanessian, G. *J. Am. Chem. Soc.* **2004**, *126*, 1836–1842.
- (9) Wincel, H. *J. Phys. Chem. A* **2007**, *111*, 5784–5791.

- (10) Jockusch, R. A.; Price, W. D.; Williams, E. R. *J. Phys. Chem. A* **1999**, *103*, 9266–9274.
- (11) Talley, J. M.; Cerda, B. A.; Ohanessian, G.; Wesdemiotis, C. *Chem.—Eur. J.* **2002**, *8*, 1377–1388.
- (12) Cerda, B. A.; Wesdemiotis, C. *Analyst* **2000**, *125*, 657–660.
- (13) Bush, M. F.; O'Brien, J. T.; Prell, J. S.; Saykally, R. J.; Williams, E. R. *J. Am. Chem. Soc.* **2007**, *129*, 1612–1622.
- (14) Forbes, M. W.; Bush, M. F.; Polfer, N. C.; Oomens, J.; Dunbar, R. C.; Williams, E. R. *J. Phys. Chem. A* **2007**, *111*, 11759–11770.
- (15) Bush, M. F.; Forbes, M. W.; Jockusch, R. A.; Oomens, J.; Polfer, N. C.; Saykally, R. J.; Williams, E. R. *J. Phys. Chem. A* **2007**, *111*, 7753–7760.
- (16) Wyttenbach, T.; Witt, M.; Bowers, M. T. *J. Am. Chem. Soc.* **2000**, *122*, 3458–3464.
- (17) Ding, Y. B.; Krogh-Jespersen, K. *Chem. Phys. Lett.* **1992**, *199*, 261–266.

beryllium, is calculated to be zwitterionic.^{18–22} Nonzwitterionic glycine is lowest in energy when complexed with monovalent Co,²³ Cu,^{24–27} Fe,²⁸ Ni,²⁹ and Zn^{19,30} ions, but the zwitterionic form of glycine is lowest in energy when complexed with divalent Co,^{23,31} Cu,^{22,25,31} Fe,^{28,31} Ni,^{22,31} and Zn^{22,30–32} ions. The structure of cysteine complexed with divalent transition metal ions is dependent on metal identity; nonzwitterionic structures are calculated to be lowest in energy for Zn²⁺ and Cd²⁺, whereas zwitterionic structures are lowest in energy for Cu²⁺ and Hg²⁺.³³

There have been very few experimental studies probing the structures of the amino acids complexed with divalent metal ions. Collisional activation of glycine complexed with divalent calcium yields fragments consistent with reactions from zwitterionic glycine, although nonzwitterionic glycine may be present or formed as an intermediate.³⁴ Singly charged complexes consisting of deprotonated amino acids complexed with Zn²⁺ have been probed with collision activation³⁵ and IRMPD action spectroscopy.³⁶ Very recently, Dunbar and Oomens reported the IRMPD spectrum of divalent barium complexed with tryptophan and concluded that tryptophan is zwitterionic in this ion.³⁷

Action spectroscopy has emerged as a powerful method to directly probe gas-phase structures of cationized amino acids and amino acid analogues,^{8,13–15,37–44} peptides,^{42,45–47} amino

acid complexes,^{48–51} and proteins.^{52,53} Action spectra of gas-phase hydrogen–deuterium exchange⁵⁴ and collisionally activated dissociation⁵⁵ products have provided insights into the mechanisms of these reactions. The majority of these action spectra were acquired via IRMPD using light generated by benchtop laser systems based on nonlinear frequency conversion (typically 2.5–4 μm)^{13,40,49,52} or free electron lasers (typically 5–20 μm).^{8,14,15,37–39,42–46,50,51,53–55} Elegant doubly resonant infrared and ultraviolet spectroscopy experiments by Rizzo and co-workers recently yielded conformer-specific infrared spectra of protonated biomolecules, demonstrating the tremendous capability of this method for investigating the structures of complex biomolecules.^{41,47} Here, IRMPD action spectroscopy is used to probe the structures of Arg•Sr²⁺, Arg•Ba²⁺, Gln•Ba²⁺, Pro•Ba²⁺, Ser•Ba²⁺, and Val•Ba²⁺ and to determine the effects of alkaline earth metal ion complexation and alkaline earth metal size on zwitterion stability.

Methods

IR Action Spectroscopy. Experiments were performed using a 4.7 T Fourier-transform ion cyclotron resonance mass spectrometer combined with a tunable free electron laser.⁵⁶ The instrument and general experimental methods are described elsewhere.^{36,57} Cationized amino acids were formed by electrospray ionization from a solution of 1 mM amino acid and 1 mM alkaline earth metal nitrate or hydroxide in 80:20 MeOH/H₂O infused at a rate of 30 $\mu\text{L}/\text{min}$. For most IRMPD spectra, the photodissociation yield is the sum of the intensities of the product ions divided by the sum of the product and precursor ion intensities.^{14,42} Because precursor ion intensities for Gln•Ba²⁺ and Val•Ba²⁺ were very low, product ion intensities were also very low, resulting in spectra with poor signal-to-noise ratio (S/N). For these ions, photodissociation yields were instead determined from the precursor intensity after laser irradiation at each frequency, $[\text{AA}\cdot\text{Ba}^{2+}(\nu)]$, using the equation $-\ln([\text{AA}\cdot\text{Ba}^{2+}(\nu)]/[\text{AA}\cdot\text{Ba}^{2+}]_0)$, where $[\text{AA}\cdot\text{Ba}^{2+}]_0$ is the precursor ion intensity observed in the absence of laser irradiation. This

(18) Strittmatter, E. F.; Lemoff, A. S.; Williams, E. R. *J. Phys. Chem. A* **2000**, *104*, 9793–9796.
 (19) Hoyau, S.; Pelicier, J. P.; Rogalewicz, F.; Hoppilliard, Y.; Ohanessian, G. *Eur. J. Mass Spectrom.* **2001**, *7*, 303–311.
 (20) Ai, H. Q.; Bu, Y. X.; Li, P. *Int. J. Quantum Chem.* **2003**, *94*, 205–214.
 (21) Ai, H. Q.; Bu, Y. X.; Li, P.; Zhang, C. *New J. Chem.* **2005**, *29*, 1540–1548.
 (22) Remko, M.; Rode, B. M. *J. Phys. Chem. A* **2006**, *110*, 1960–1967.
 (23) Constantino, E.; Rodriguez-Santiago, L.; Sodupe, M.; Tortajada, J. J. *Phys. Chem. A* **2005**, *109*, 224–230.
 (24) Hoyau, S.; Ohanessian, G. *J. Am. Chem. Soc.* **1997**, *119*, 2016–2024.
 (25) Bertran, J.; Rodriguez-Santiago, L.; Sodupe, M. *J. Phys. Chem. B* **1999**, *103*, 2310–2317.
 (26) Shoeib, T.; Rodriguez, C. F.; Siu, K. W. M.; Hopkinson, A. C. *Phys. Chem. Chem. Phys.* **2001**, *3*, 853–861.
 (27) Hoppilliard, Y.; Ohanessian, G.; Bourcier, S. *J. Phys. Chem. A* **2004**, *108*, 9687–9696.
 (28) Ai, H. Q.; Bu, Y. X.; Li, P.; Li, Z. Q.; Hu, X. Q.; Chen, Z. D. *J. Phys. Org. Chem.* **2005**, *18*, 26–34.
 (29) Rodriguez-Santiago, L.; Sodupe, M.; Tortajada, J. J. *Phys. Chem. A* **2001**, *105*, 5340–5347.
 (30) Ai, H. Q.; Bu, Y. X.; Han, K. L. *J. Chem. Phys.* **2003**, *118*, 10973–10985.
 (31) Marino, T.; Toscano, M.; Russo, N.; Grand, A. *J. Phys. Chem. B* **2006**, *110*, 24666–24673.
 (32) Rogalewicz, F.; Ohanessian, G.; Gresh, N. *J. Comput. Chem.* **2000**, *21*, 963–973.
 (33) Belcastro, M.; Marino, T.; Russo, N.; Toscano, M. *J. Mass Spectrom.* **2005**, *40*, 300–306.
 (34) Corral, I.; M6, O.; Y6ñez, M.; Salpin, J. Y.; Tortajada, J.; Moran, D.; Radom, L. *Chem.—Eur. J.* **2006**, *12*, 6787–6796.
 (35) Rogalewicz, F.; Hoppilliard, Y.; Ohanessian, G. *Int. J. Mass Spectrom.* **2003**, *227*, 439–451.
 (36) Polfer, N. C.; Oomens, J.; Moore, D. T.; von Helden, G.; Meijer, G.; Dunbar, R. C. *J. Am. Chem. Soc.* **2006**, *128*, 517–525.
 (37) Dunbar, R. C.; Polfer, N. C.; Oomens, J. *J. Am. Chem. Soc.* **2007**, *129*, 14562–14563.
 (38) Simon, A.; MacAleese, L.; M6itre, P.; Lemaire, J.; McMahon, T. B. *J. Am. Chem. Soc.* **2007**, *129*, 2829–2840.
 (39) Polfer, N. C.; Oomens, J.; Dunbar, R. C. *Phys. Chem. Chem. Phys.* **2006**, *8*, 2744–2751.
 (40) Kamariotis, A.; Boyarkin, O. V.; Mercier, S. R.; Beck, R. D.; Bush, M. F.; Williams, E. R.; Rizzo, T. R. *J. Am. Chem. Soc.* **2006**, *128*, 905–916.
 (41) Stearns, J. A.; Mercier, S.; Seaiby, C.; Guidi, M.; Boyarkin, O. V.; Rizzo, T. R. *J. Am. Chem. Soc.* **2007**, *129*, 11814–11820.

(42) Polfer, N. C.; Paizs, B.; Snoek, L. C.; Compagnon, I.; Suhai, S.; Meijer, G.; von Helden, G.; Oomens, J. *J. Am. Chem. Soc.* **2005**, *127*, 8571–8579.
 (43) Rodgers, M. T.; Armentrout, P. B.; Oomens, J.; Steill, J. D. *J. Phys. Chem. A* **2008**, *112*, 2248–2257.
 (44) Armentrout, P. B.; Rodgers, M. T.; Oomens, J.; Steill, J. D. *J. Phys. Chem. A* **2008**, *112*, 2258–2267.
 (45) Balaj, O.-P.; Kapota, C.; Lemaire, J.; Ohanessian, G. *Int. J. Mass Spectrom.* **2008**, *269*, 196–209.
 (46) Wu, R.; McMahon, T. B. *J. Am. Chem. Soc.* **2007**, *129*, 11312–11313.
 (47) Stearns, J. A.; Boyarkin, O. V.; Rizzo, T. R. *J. Am. Chem. Soc.* **2007**, *129*, 13820–13821.
 (48) Oh, H. B.; Lin, C.; Hwang, H. Y.; Zhai, H. L.; Breuker, K.; Zabriskov, V.; Carpenter, B. K.; McLafferty, F. W. *J. Am. Chem. Soc.* **2005**, *127*, 4076–4083.
 (49) Kong, X. L.; Tsai, I. A.; Sabu, S.; Han, C. C.; Lee, Y. T.; Chang, H. C.; Tu, S. Y.; Kung, A. H.; Wu, C. C. *Angew. Chem., Int. Ed.* **2006**, *45*, 4130–4134.
 (50) Wu, R. H.; McMahon, T. B. *J. Am. Chem. Soc.* **2007**, *129*, 4864–4865.
 (51) Rajabi, K.; Fridgen, T. D. *J. Phys. Chem. A* **2007**, *112*, 23–30.
 (52) Oh, H.; Breuker, K.; Sze, S. K.; Ge, Y.; Carpenter, B. K.; McLafferty, F. W. *Proc. Natl. Acad. Sci. U.S.A.* **2002**, *99*, 15863–15868.
 (53) Oomens, J.; Polfer, N.; Moore, D. T.; van der Meer, L.; Marshall, A. G.; Eyler, J. R.; Meijer, G.; von Helden, G. *Phys. Chem. Chem. Phys.* **2005**, *7*, 1345–1348.
 (54) Polfer, N. C.; Dunbar, R. C.; Oomens, J. *J. Am. Soc. Mass Spectrom.* **2007**, *18*, 512–516.
 (55) Polfer, N. C.; Oomens, J.; Suhai, S.; Paizs, B. *J. Am. Chem. Soc.* **2007**, *129*, 5887–5897.
 (56) Oepds, D.; van der Meer, A. F. G.; van Amersfoort, P. W. *Infrared Phys. Technol.* **1995**, *36*, 297–308.
 (57) Valle, J. J.; Eyler, J. R.; Oomens, J.; Moore, D. T.; van der Meer, A. F. G.; von Helden, G.; Meijer, G.; Hendrickson, C. L.; Marshall, A. G.; Blakney, G. T. *Rev. Sci. Instrum.* **2005**, *76*, 023103.

results in spectra with improved S/N because noise associated with low abundance fragment ions do not contribute to the spectra.

Computational Chemistry. Initial structures of $\text{AA}\cdot\text{M}^{2+}$, where AA = amino acid and M = alkaline earth metal, were generated by Monte Carlo conformational searching using the MMFFs (M = Mg and Ca) and OPLS2005 (M = Ba) force fields as implemented in MacroModel v. 8.1 (Schrödinger, Inc., Portland, OR). Additional structures were obtained by substituting metal ions in these structures and those reported previously for alkali metal cationized arginine.¹³ The resulting low-energy structures were grouped into families with similar noncovalent interactions. Representative structures from each family were energy-minimized using hybrid method density functional calculations (B3LYP) as implemented in Jaguar v. 6.5 (Schrödinger, Inc., Portland, OR) using the LANL2DZ effective core potential for Ca, Sr, and Ba, and the 6-31G(p,d) basis set for all remaining elements.

The lowest-energy structure in each family was energy-minimized, and vibrational frequencies were calculated using the SRSC effective core potential (ECP) for Sr,⁵⁸ the CRENBL ECP for Ba,⁵⁹ and the 6-31+G(p,d) basis set for all remaining elements as implemented in Q-Chem v. 3.0.⁶⁰ All frequencies were scaled by 0.975 (vide infra) and broadened using 40 cm^{-1} fwhm Gaussian distributions. Vibrational analysis of most structures yielded all positive frequency vibrational modes. For the **NO**–**NZ** structure of $\text{Val}\cdot\text{Ba}^{2+}$, the **O_AO_C**–**ZW** structure of $\text{Gln}\cdot\text{Ba}^{2+}$, and the **OO**-coordinated structure of $[\text{Val} - \text{H} + \text{Ba}]^+$, convergence to a gradient of less than 1×10^{-6} (default gradient threshold for geometry optimization = 3×10^{-4}) yielded one imaginary frequency of magnitude $\leq 70 \text{ cm}^{-1}$, indicative of a torsional mode on a very flat region of the potential energy surface or artifacts in the computational method. The imaginary vibrational frequency modes were ignored in calculating thermochemical corrections, and this approximation should contribute negligibly to the uncertainties in these calculations. Relative free energies are reported from B3LYP/6-311++G(2d,2p) and MP2/6-311++G(2d,2p) single point energies using geometries and temperature corrections determined at the B3LYP/6-31+G(d,p) level of theory and the ECPs identified above.

Results and Discussion

IRMPD action spectra of $\text{Arg}\cdot\text{Sr}^{2+}$, $\text{Arg}\cdot\text{Ba}^{2+}$, $\text{Gln}\cdot\text{Ba}^{2+}$, $\text{Pro}\cdot\text{Ba}^{2+}$, $\text{Ser}\cdot\text{Ba}^{2+}$, and $\text{Val}\cdot\text{Ba}^{2+}$ are shown in Figure 1. Information about the structures of these complexes is inferred from comparisons with IRMPD spectra of alkali metal cationized amino acids, each other, and with calculated absorbance spectra for candidate structures of these ions.

Structure of $\text{Pro}\cdot\text{Ba}^{2+}$. Barium can coordinate to either the N-terminal amino group and an oxygen atom of the carboxylic acid group of nonzwitterionic proline, **NO**–**NZ**, or to both oxygen atoms of the carboxylate group of zwitterionic proline, **OO**–**ZW** (Figure 2). Structures in which the metal ion coordinates to both oxygen atoms of the carboxylic acid group of nonzwitterionic proline, analogous to the lowest-energy structure of many aliphatic amino acids complexed with larger alkali metal ions,^{19,61} are not stable and energy minimize to **OO**–**ZW**. Similar results have been reported for glycine complexed with alkaline earth metal ions.^{18,19} Structures in which the metal ion coordinates to a single oxygen atom of the carboxylic acid group of nonzwitterionic proline were not considered because these structures were found to be $\sim 100 \text{ kJ}$ /

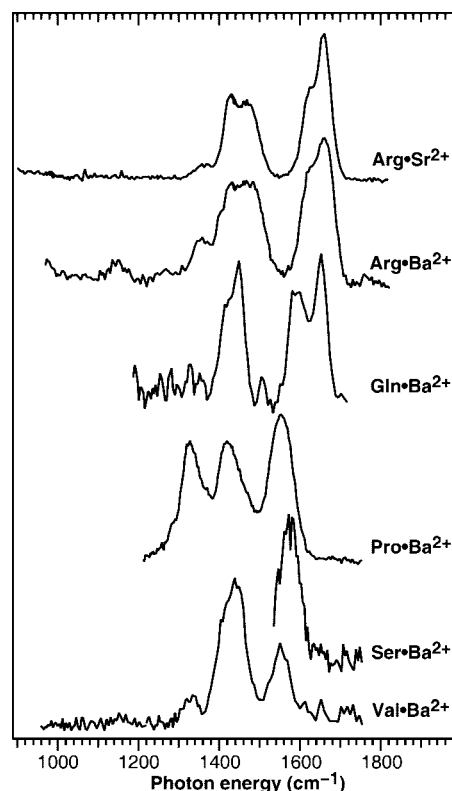


Figure 1. IRMPD spectra of $\text{Arg}\cdot\text{Sr}^{2+}$, $\text{Arg}\cdot\text{Ba}^{2+}$, $\text{Gln}\cdot\text{Ba}^{2+}$, $\text{Pro}\cdot\text{Ba}^{2+}$, $\text{Ser}\cdot\text{Ba}^{2+}$, and $\text{Val}\cdot\text{Ba}^{2+}$. The photodissociation intensities for $\text{Gln}\cdot\text{Ba}^{2+}$ and $\text{Val}\cdot\text{Ba}^{2+}$ are determined from depletion of the precursor ion, whereas those for the remaining ions are determined from the relative abundance of the precursor and product ions. The spectrum of $\text{Gln}\cdot\text{Ba}^{2+}$ has been smoothed.

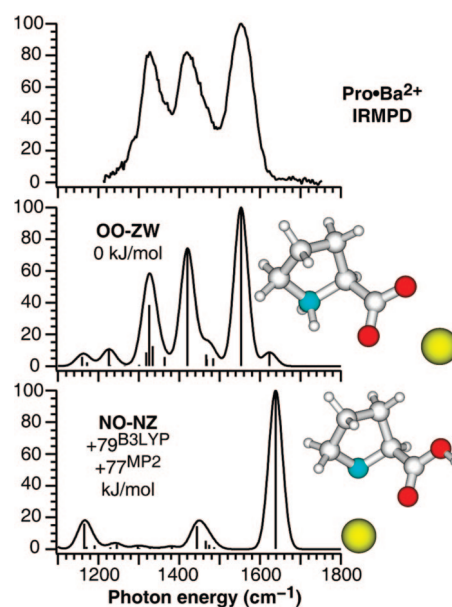


Figure 2. IRMPD spectrum and calculated absorbance spectra for two low-energy structures of $\text{Pro}\cdot\text{Ba}^{2+}$. Relative B3LYP/6-311++G(2d,2p)//6-31+G(d,p) and MP2/6-311++G(2d,2p)//B3LYP/6-31+G(d,p) free energies at 298 K are reported for each conformer.

mol higher in energy than **NO**–**NZ** for glycine complexed with the alkaline earth metal ions.¹⁸

The IRMPD spectrum of $\text{Pro}\cdot\text{Ba}^{2+}$ contains strong bands at 1320, 1420, and 1550 cm^{-1} that are similar in frequency to the

- (58) Kaupp, M.; Schleyer, P. v. R.; Stoll, H.; Preuss, H. *J. Chem. Phys.* **1991**, *94*, 1360–1366.
 (59) Ross, R. B.; Powers, J. M.; Atashroo, T.; Ermler, W. C.; Lajohn, L. A.; Christiansen, P. A. *J. Chem. Phys.* **1990**, *93*, 6654–6670.
 (60) Shao, Y.; et al. *Phys. Chem. Chem. Phys.* **2006**, *8*, 3172–3191.
 (61) Jockusch, R. A.; Lemoff, A. S.; Williams, E. R. *J. Am. Chem. Soc.* **2001**, *123*, 12255–12265.

bonded NH bend (1326 cm^{-1} , also coupled with CH bending modes), carboxylate symmetric stretch (1421 cm^{-1}), and carboxylate asymmetric stretch (1553 cm^{-1}), respectively, calculated for structure **OO-ZW**. In contrast, the most intense bands in this region calculated for structure **NO-NZ** correspond to the OH bend (1165 cm^{-1}) and the symmetric (1444 cm^{-1}) and asymmetric (1638 cm^{-1}) stretches of the carboxylic acid group and thus provide very poor agreement with the experimental spectrum. Therefore, the absence of additional bands centered at frequencies greater than 1550 cm^{-1} and the absence of measurable photodissociation at frequencies greater than 1640 cm^{-1} ostensibly limits the possibility that any nonzwitterionic structures contribute to the observed IRMPD spectrum. Finally, structure **NO-NZ** is calculated to be 77 to 79 kJ/mol higher in energy than structure **OO-ZW**. Therefore, comparisons between the experimental action spectrum and the calculated vibrational spectra and the calculated energies both provide compelling evidence that proline is zwitterionic when complexed with barium.

Calculations and a variety of experiments indicate that $\text{Pro}\cdot\text{Na}^+$ adopts a structure analogous to **OO-ZW** for $\text{Pro}\cdot\text{Ba}^{2+}$.^{2,3,7,8} In the IRMPD spectrum of $\text{Pro}\cdot\text{Na}^+$, the carboxylate asymmetric stretch occurs at 1698 cm^{-1} , whereas the bonded NH bend (calculated to couple with CH bends and occur between 1319 and 1384 cm^{-1}) and carboxylate symmetric stretch (calculated to occur near 1400 cm^{-1}) are superimposed and appear as a broad band ranging from 1306 to 1429 cm^{-1} .⁸ The carboxylate asymmetric stretch for $\text{Pro}\cdot\text{Ba}^{2+}$ is red-shifted by $\sim 150\text{ cm}^{-1}$ compared to that for $\text{Pro}\cdot\text{Na}^+$, consistent with substantially greater charge transfer from the carboxylate group to the doubly charged metal ion. Because the bonded NH bend and carboxylate symmetric stretch were not resolved for $\text{Pro}\cdot\text{Na}^+$,⁸ comparing the frequencies of these bands is challenging. However, these resolved bands for $\text{Pro}\cdot\text{Ba}^{2+}$ do occur in the frequency region of the unresolved band for $\text{Pro}\cdot\text{Na}^+$, suggesting that the frequency of these modes may be less sensitive to the charge state of the ion than the carboxylate asymmetric stretch.

The carboxylate asymmetric stretch for $\text{Pro}\cdot\text{Ba}^{2+}$ is centered near 1550 cm^{-1} , whereas the corresponding band for tryptophan (Trp) complexed with barium is centered near 1600 cm^{-1} .³⁷ The relative position of this mode for $\text{Trp}\cdot\text{Ba}^{2+}$ is consistent with cation- π interactions between barium and the tryptophan side chain and decreased charge transfer from the carboxylate group to the barium ion.

Structure of $\text{Val}\cdot\text{Ba}^{2+}$. The IRMPD spectrum for $\text{Val}\cdot\text{Ba}^{2+}$ contains a band near 1550 cm^{-1} , identical to that assigned to the carboxylate asymmetric stretch for $\text{Pro}\cdot\text{Ba}^{2+}$ and very close in frequency to that calculated for this mode of structure **OO-ZW** (1562 cm^{-1} , Figure 3). An intense band near 1440 cm^{-1} is attributable to the carboxylate symmetric stretch (1428 cm^{-1}) and the protonated amine umbrella bend (1488 cm^{-1}). Note that this band is close in frequency to the most intense band in the IRMPD spectrum of $\text{Trp}\cdot\text{Ba}^{2+}$ (1450 cm^{-1}), which was assigned to the protonated amine umbrella bend of that ion.³⁷ The spectrum calculated for structure **NO-NZ** of $\text{Val}\cdot\text{Ba}^{2+}$ is dominated by an intense band at 1628 cm^{-1} corresponding to the carbonyl stretch of the carboxylic acid group of that ion. The IRMPD spectrum of $\text{Val}\cdot\text{Ba}^{2+}$ exhibits very little photodissociation intensity at frequencies greater than 1600 cm^{-1} . This indicates that the structure of $\text{Val}\cdot\text{Ba}^{2+}$ is most consistent with **OO-ZW**, and it appears that the protonated

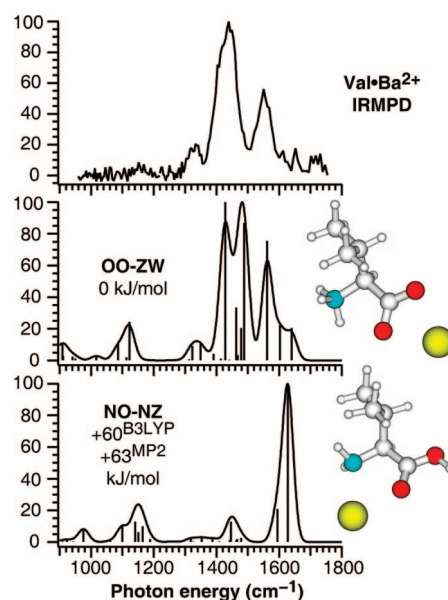


Figure 3. IRMPD spectrum and calculated absorbance spectra for two low-energy structures of $\text{Val}\cdot\text{Ba}^{2+}$. Relative B3LYP/6-311++G(2d,2p)//6-31+G(d,p) and MP2/6-311++G(2d,2p)//B3LYP/6-31+G(d,p) free energies at 298 K are reported for each conformer.

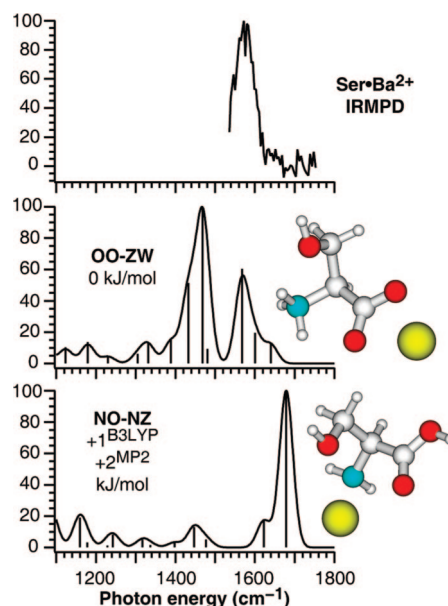


Figure 4. IRMPD spectrum and calculated absorbance spectra for four low-energy structures of $\text{Ser}\cdot\text{Ba}^{2+}$. Relative B3LYP/6-311++G(2d,2p)//6-31+G(d,p) and MP2/6-311++G(2d,2p)//B3LYP/6-31+G(d,p) free energies at 298 K are reported for each conformer.

amine umbrella bend and carboxylate symmetric stretch are superimposed in the experimental spectrum.

Structure of $\text{Ser}\cdot\text{Ba}^{2+}$. The IRMPD spectrum for $\text{Ser}\cdot\text{Ba}^{2+}$ measured over a limited frequency range is shown in Figure 4. The absence of photodissociation at frequencies greater than $\sim 1620\text{ cm}^{-1}$, a spectral signature for a carboxylic acid functional group, and the presence of an intense band near 1570 cm^{-1} , essentially identical to the calculated frequency of the asymmetric stretch of the carboxylate group of zwitterionic $\text{Ser}\cdot\text{Ba}^{2+}$ (**OO-ZW**, 1568 cm^{-1}), indicate that serine is zwitterionic in this ion. The frequency of the carboxylate asymmetric stretch of $\text{Ser}\cdot\text{Ba}^{2+}$ is slightly blue-shifted from those exhibited by $\text{Pro}\cdot\text{Ba}^{2+}$ and $\text{Val}\cdot\text{Ba}^{2+}$, which may be

attributable to less charge transfer from the carboxylate group to the protonated amine group that is solvated by the side chain hydroxyl group for $\text{Ser}\cdot\text{Ba}^{2+}$ or perhaps an inductive effect from the side chain.

Interestingly, structures **NO–NZ** and **OO–ZW** of $\text{Ser}\cdot\text{Ba}^{2+}$ are calculated to be essentially isoenergetic. Compared to valine, the nonzwitterionic structure is preferentially stabilized by the short alcohol side chain of serine that solvates the metal ion in the **NO–NZ** structure. Zwitterionic structures in which the metal ion is solvated with the oxygen atoms of the alcohol and carboxylate functional groups energy minimize to **OO–ZW**. Furthermore, if the side chain of serine solvates barium in this ion, the carboxylate asymmetric stretch would be expected to be further blue-shifted from that calculated for structure **OO–ZW** and be closer in frequency to that observed for $\text{Trp}\cdot\text{Ba}^{2+}$ (1600 cm^{-1}),³⁷ in which the metal ion is solvated by the tryptophan side chain. These results provide strong evidence that serine is zwitterionic when complexed with barium and that the side chain solvates the protonated amino group rather than the divalent metal ion.

Structure of $\text{Gln}\cdot\text{Ba}^{2+}$. The IRMPD spectrum of $\text{Gln}\cdot\text{Ba}^{2+}$ is shown in Figure 5. The low S/N of the spectrum is attributable to low precursor ion abundance, and averaging the precursor depletion at each frequency with those of the nearest neighbors makes bands near 1430 , 1590 , and 1650 cm^{-1} more readily apparent. Data smoothing is applied to frequency ranges ($7\text{--}15\text{ cm}^{-1}$) that are substantially less than the bandwidths exhibited in these IRMPD spectra. Four candidate low-energy structures were identified for $\text{Gln}\cdot\text{Ba}^{2+}$ and are shown in Figure 5. These structures are a subset of those identified for alkali metal cationized glutamine in which the divalent barium ion is most solvated by a combination of the polarizable amino nitrogen (N), the carbonyl oxygen of the amide side chain (O_A), and one (O_C) or two (OO_C) oxygen atoms of the carboxylic acid/carboxylate functional group.⁶² The remaining structures identified for alkali metal cationized glutamine favor hydrogen bond formation over charge solvation; these structures energy minimize to the four structures discussed above or are significantly higher in energy for alkaline earth metal cationized glutamine.

In addition to the bands discussed previously for $\text{Pro}\cdot\text{Ba}^{2+}$, $\text{Ser}\cdot\text{Ba}^{2+}$, and $\text{Val}\cdot\text{Ba}^{2+}$, the high-frequency region of this IRMPD spectrum also has bands originating from the amide group of the glutamine side chain. For calculated structures in which the amide group solvates the metal ion, the NH_2 bend and carbonyl stretch of the amide side chain are calculated to occur from 1572 to 1580 cm^{-1} and 1647 to 1653 cm^{-1} , respectively. For **OO_C–ZW**, in which the amide group solvates the protonated amine group, these modes are calculated to occur at $1593\text{--}1602$ (a pair of coupled oscillators) and 1682 cm^{-1} , respectively. The blue shift of these bands for the latter structure is attributable to reduced charge transfer from the amide group to the protonated amine group. These calculations suggest that the IRMPD bands at 1590 and 1650 cm^{-1} can be attributed to, or contain contributions from, the NH_2 bend and carbonyl stretch of the amide side chain, respectively. Additionally, the low frequency of the latter band indicates that the side chain solvates the metal ion. The band position of the NH_2 bend for the amide group is observed at frequencies similar to those calculated for all four candidate structures, and it is therefore difficult to draw any additional structural conclusions from this band.

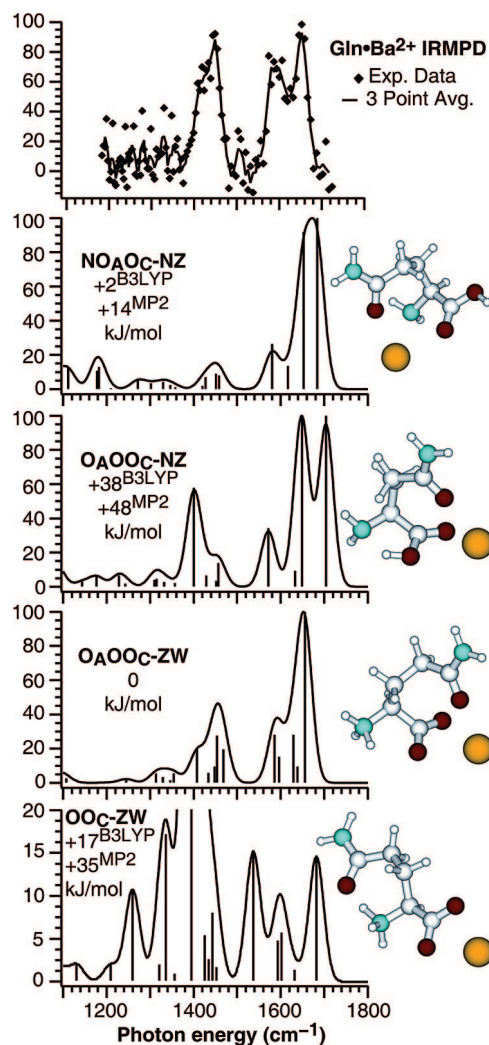


Figure 5. IRMPD spectrum and calculated absorbance spectra for four low-energy structures of $\text{Gln}\cdot\text{Ba}^{2+}$. Calculated intensities for **OO_C–ZW** are expanded by a factor of 5 because the coupled bonded NH bending and carboxylate symmetric stretching mode for this structure is ~ 3 times more intense than any other calculated oscillator in this study. Relative B3LYP/6-311++G(2d,2p)//6-31+G(d,p) and MP2/6-311++G(2d,2p)//B3LYP/6-31+G(d,p) free energies at 298 K are reported for each conformer.

The carbonyl stretches of the carboxylic acid groups of structures **NOAOC–NZ** and **OAOOC–NZ** of $\text{Gln}\cdot\text{Ba}^{2+}$ are calculated to occur at 1684 and 1704 cm^{-1} , respectively. These calculated frequencies are substantially blue-shifted from those calculated for the nonzwitterionic forms of $\text{Pro}\cdot\text{Ba}^{2+}$ and $\text{Val}\cdot\text{Ba}^{2+}$, consistent with solvation of the divalent metal ion by the glutamine side chain. The lack of IRMPD bands centered at frequencies greater than 1650 cm^{-1} ostensibly limits the possibility that structures with carboxylic acid groups are present under the conditions of the experiment, that is, $\text{Gln}\cdot\text{Ba}^{2+}$ is zwitterionic.

Three important types of oscillators calculated for structure **OAOOC–ZW**, the carboxylate symmetric stretch (1398 cm^{-1}), protonated amine umbrella bends (pair of coupled oscillators at 1451 and 1464 cm^{-1}), and carboxylate asymmetric stretch (pair of coupled oscillators at 1596 and 1629 cm^{-1}), all occur at frequencies consistent with the IRMPD spectrum of the ion. The fit to structure **OO_C–ZW** is significantly poorer due to the positions of the amide carbonyl stretch (vide supra), the frequency calculated for the carboxylate asymmetric stretch

(62) Lemoff, A. S.; Bush, M. F.; Wu, C. C.; Williams, E. R. *J. Am. Chem. Soc.* **2005**, *127*, 10276–10286.

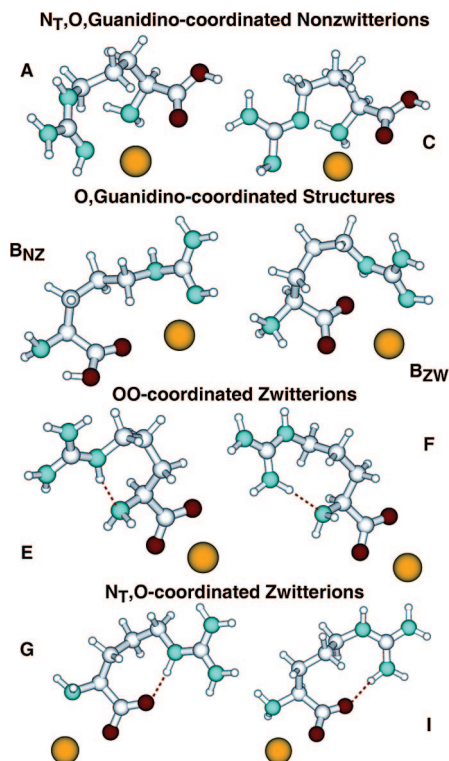


Figure 6. Low-energy structures of $\text{Arg}\cdot\text{Ba}^{2+}$ optimized at the B3LYP/6-31+G(d,p) level of theory. Low-energy structures of $\text{Arg}\cdot\text{Ca}^{2+}$ are shown in Supporting Information Figure 1.

(1537 cm^{-1} , a frequency exhibiting little photodissociation), and the large mismatch of relative oscillator intensities between the bands above and below 1500 cm^{-1} . Comparisons with the absorbance spectra calculated for candidate structures indicate that $\text{Gln}\cdot\text{Ba}^{2+}$ is zwitterionic and that the amide side chain solvates the metal ion. These conclusions are consistent with structure $\text{O}_A\text{OO}_C\text{-ZW}$, although other similar structures cannot be discounted.

Low-Energy Structures of $\text{Arg}\cdot\text{M}^{2+}$. The low-energy non-zwitterionic and zwitterionic structures identified for $\text{Arg}\cdot\text{M}^{2+}$ are similar for all M, where M = alkaline earth metal, and those for M = Ba are shown in Figure 6 (for comparison, structures for M = Ca are shown in Supporting Information Figure 1). The majority of these structures are a subset of those identified for $\text{Arg}\cdot\text{M}^+$, M = alkali metal, and are labeled according to the designations reported previously.^{13,14} One new low-energy zwitterionic structure was identified in which the N-terminal amino group is protonated instead of the guanidino side chain (B_{ZW}). For analogous ions containing alkali metal ions, this structure energy minimizes to nonzwitterionic structure B_{NZ} . Zwitterionic forms in which the carboxylate group interacts with both the guanidinium side chain and the metal ion (**D**, **H**, and **J**) are unstable and energy minimize to structures in which the guanidinium side chain does not interact with the carboxylate group; the metal ion and the charged side chain are spatially separated in all energy-minimized zwitterionic structures investigated. The geometries of these low-energy zwitterionic structures (**E–G** and **I**) and nonzwitterionic structure **A** are remarkably similar for both $\text{Arg}\cdot\text{M}^+$ and $\text{Arg}\cdot\text{M}^{2+}$. In contrast, the geometries for structures B_{NZ} and **C** differ for complexes of the two charge states. For these structures of $\text{Arg}\cdot\text{M}^+$, the nitrogen atoms in the guanidino side chains are trigonal planar, whereas some of those for $\text{Arg}\cdot\text{M}^{2+}$ are significantly more

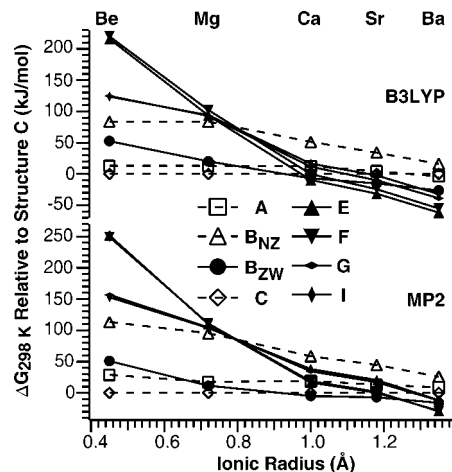


Figure 7. Relative B3LYP/6-311++G(2d,2p)//6-31+G(d,p) and MP2/6-311++G(2d,2p)//B3LYP/6-31+G(d,p) free energies at 298 K for $\text{Arg}\cdot\text{M}^{2+}$, M = alkaline earth metal, conformers versus ionic radii.⁶⁴

tetrahedral. This suggests that the guanidino group for $\text{Arg}\cdot\text{M}^+$ is conjugated, whereas the guanidino group for $\text{Arg}\cdot\text{M}^{2+}$ transfers significant electron density to the metal ion and is partially deconjugated.

The relative free energies of these structures have a strong dependence on metal ion size. These values calculated at two different levels of theory are plotted as a function of metal ion size in Figure 7 and are reported in Supporting Information Table 1. The calculated results at both levels of theory clearly indicate that zwitterionic forms of $\text{Arg}\cdot\text{M}^{2+}$ are increasingly stable with increasing alkaline earth metal ion size, analogous to trends established for alkali metal cationized arginine.^{10,12–14} At the B3LYP/6-311++G(2d,2p)//6-31+G(d,p) level of theory, the lowest-energy forms of $\text{Arg}\cdot\text{Be}^{2+}$ and $\text{Arg}\cdot\text{Mg}^{2+}$ are nonzwitterionic, whereas those of $\text{Arg}\cdot\text{Sr}^{2+}$ and $\text{Arg}\cdot\text{Ba}^{2+}$ are zwitterionic. The nonzwitterionic and zwitterionic forms of $\text{Arg}\cdot\text{Ca}^{2+}$ are close in energy at this level of theory. At the MP2/6-311++G(2d,2p)//B3LYP/6-31+G(d,p) level of theory, nonzwitterionic structures and zwitterionic structures with protonated N-terminal amino groups (B_{ZW}) are preferentially stabilized relative to the zwitterionic structures with protonated side chains (**E–G** and **I**).

For all M, the two nonzwitterionic forms in which the metal ion is solvated by the N-terminal amino group (N_T), the carbonyl oxygen, and the side chain (**A** and **C**) are close in relative free energies, as are those of the two **OO**-coordinated zwitterions (**E** and **F**) and those of the two N_TO -coordinated zwitterions (**G** and **I**). Structure B_{NZ} is always at least 30 kJ/mol higher in free energy than B_{ZW} . Structure **C** is the lowest-energy nonzwitterionic structure for all M at the MP2/6-311++G(2d,2p)//B3LYP/6-31+G(d,p) level of theory. With increasing alkaline earth metal ion size, structure **A** is preferentially stabilized relative to structure **C** and the former is lower in energy for $\text{Arg}\cdot\text{Ba}^{2+}$ at the B3LYP/6-311++G(2d,2p)//6-31+G(d,p) level of theory. Structure B_{ZW} is the lowest-energy zwitterionic structure for M = Be and Mg at the B3LYP/6-311++G(2d,2p)//6-31+G(d,p) level of theory and M = Be, Mg, Ca, and Sr at the MP2/6-311++G(2d,2p)//B3LYP/6-31+G(d,p) level of theory, but increasing metal ion size preferentially stabilizes the other zwitterionic forms of the amino acid to a tremendous extent and **OO**-coordinated zwitterions (**E** and **F**) are the lowest-energy zwitterionic structures for all other ions.

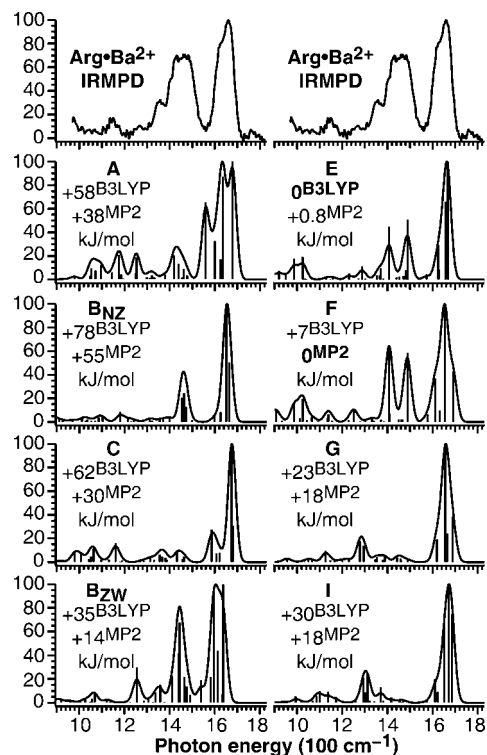


Figure 8. IRMPD spectrum and calculated absorbance spectra for eight low-energy structures of $\text{Arg}\cdot\text{Ba}^{2+}$. Relative B3LYP/6-311++G(2d,2p)//6-31+G(d,p) and MP2/6-311++G(2d,2p)//B3LYP/6-31+G(d,p) free energies at 298 K are reported for each conformer. Data for $\text{Arg}\cdot\text{Sr}^{2+}$ are shown in Supporting Information Figure 2.

Structures of $\text{Arg}\cdot\text{Sr}^{2+}$ and $\text{Arg}\cdot\text{Ba}^{2+}$. The IRMPD spectra of $\text{Arg}\cdot\text{Sr}^{2+}$ and $\text{Arg}\cdot\text{Ba}^{2+}$ are nearly the same, indicating that these ions have similar structures. The following discussion focuses primarily on $\text{M} = \text{Ba}$, but equivalent arguments can be made for $\text{M} = \text{Sr}$. Inspection of the calculated absorbance spectra in Figure 8 reveals that interpretation of these IRMPD spectra is more complicated than that for $\text{Gln}\cdot\text{Ba}^{2+}$, $\text{Pro}\cdot\text{Ba}^{2+}$, $\text{Ser}\cdot\text{Ba}^{2+}$, and $\text{Val}\cdot\text{Ba}^{2+}$. For example, assigning the higher frequency band centered near 1650 cm^{-1} is challenging due to spectral congestion and because both nonzwitterionic and zwitterionic structures are calculated to have bands in this region. Although the IRMPD spectra of alkali metal cationized arginine were also congested in this region, the structurally diagnostic carboxylic acid carbonyl stretches for the nonzwitterionic structures were both calculated and observed at higher frequencies in an uncongested region of the spectrum.¹⁴ For nonzwitterionic structures **A** and **C** of $\text{Arg}\cdot\text{Ba}^{2+}$, this mode is calculated to occur from 1674 to 1679 cm^{-1} , which is on the blue edge of the IRMPD band. For structure **BNZ**, this mode is calculated to occur near the center of the observed band (1651 cm^{-1}). In all cases, multiple NH bending modes are also calculated to occur in this region for both the nonzwitterionic and zwitterionic structures, which greatly complicates establishing the presence or absence of nonzwitterionic structures.

However, there are substantial differences between the IRMPD spectrum and some of the calculated spectra. The IRMPD spectrum exhibits intense, albeit broad, photodissociation in the region centered near 1450 cm^{-1} , but structures **A**, **C**, **G**, and **I** are calculated to only weakly absorb in this region. The IRMPD spectrum exhibits very little photodissociation near 1550 cm^{-1} , but structure **A** is calculated to have an intense oscillator at 1558 cm^{-1} that corresponds to the $\text{C}=\text{N}^{\text{H}}$

stretching mode of the guanidino group. On the basis of visual inspection, the spectra calculated for structures **BNZ**, **BZW**, **E**, and **F** are generally consistent with the experimental spectrum. For $\text{M} = \text{Ba}$, structures **E** and **F** are calculated to be lowest in free energy of all of the candidate structures and appear to be the best matches to the experimental spectrum. Structure **BZW** is 13 – 35 kJ/mol higher in free energy than structures **E** and **F** depending on the level of theory, and the calculated high-frequency oscillators are roughly 50 cm^{-1} red-shifted from the highest-frequency IRMPD band. Structure **BNZ** is calculated to be 43 – 78 kJ/mol higher in free energy than structures **E** and **F** depending on the level of theory, and the calculated absorbance spectrum does not account for the structure and relative intensity of the broad IRMPD band between 1350 and 1500 cm^{-1} . On the basis of the calculated free energies and comparisons between the IRMPD spectrum and the calculated absorbance spectra, the IRMPD spectrum of $\text{Arg}\cdot\text{Ba}^{2+}$ is most consistent with structures **E** and **F**. In both of these structures, arginine is zwitterionic and Ba^{2+} is solvated by both oxygen atoms of the carboxylate groups.

Carboxylate symmetric and asymmetric stretch bands are key spectroscopic signatures for the zwitterionic forms of $\text{AA}\cdot\text{Ba}^{2+}$, $\text{AA} = \text{Gln}$, Val , Pro , Ser , and Val . These modes for zwitterionic structures **E**–**G** and **I** of $\text{Arg}\cdot\text{Ba}^{2+}$ are calculated to occur at very different frequencies than those observed and calculated for ions containing the other amino acids investigated in this study. For structures **E**–**F**, the carboxylate symmetric and asymmetric stretches are calculated to occur at 1407 and 1489 – 1490 cm^{-1} , respectively, whereas those for **G** and **I** of this ion are calculated to occur at 1278 – 1312 and 1687 – 1688 cm^{-1} , respectively. The IRMPD spectra of $\text{Arg}\cdot\text{Sr}^{2+}$ and $\text{Arg}\cdot\text{Ba}^{2+}$ contain intense, albeit poorly resolved, bands centered near 1430 and 1470 cm^{-1} that are consistent with the symmetric and asymmetric stretches of the **OO**-coordinated zwitterionic structures (**E** and **F**). The spectra exhibit only minor photodissociation below 1300 cm^{-1} , indicating that **NT**O-coordinated zwitterionic structures (**G** and **I**), which are calculated to have carboxylate symmetric stretches in this region, are not predominant under the conditions of the experiment. However, the observation of a weak band to the blue of the region (1360 cm^{-1}) may be attributable to these modes and indicate the presence of small populations of **NT**O-coordinated zwitterionic structures.

The large differences in carboxylate symmetric and asymmetric stretch frequencies for zwitterionic structures **E**–**G** and **I** of $\text{Arg}\cdot\text{Ba}^{2+}$ versus the remaining $\text{AA}\cdot\text{Ba}^{2+}$ ions studied may be attributable to differences in the sites of protonation. The N-terminal amino group is the preferred site of protonation in most zwitterionic amino acids, but the side chain is protonated in zwitterionic structures **E**–**G** and **I** of $\text{Arg}\cdot\text{Ba}^{2+}$. Deprotonated valine complexed with divalent barium, $[\text{Val} - \text{H} + \text{Ba}]^+$, which contains both a carboxylate group and a neutral N-terminal amino group, provides an interesting comparison with structures **E**–**G** and **I** of $\text{Arg}\cdot\text{Ba}^{2+}$ (Figures 8 and 9). Structure **OO** of $[\text{Val} - \text{H} + \text{Ba}]^+$, in which the metal ion is solvated by both oxygen atoms of the carboxylate group, is likely a good analogue for the **OO**-coordinated zwitterionic structures of $\text{Arg}\cdot\text{Ba}^{2+}$ (**E** and **F**). The symmetric and asymmetric stretches of the carboxylate group for this ion are calculated to occur at 1445 and 1458 cm^{-1} , respectively, frequencies that are between those calculated for the **OO**-coordinated zwitterionic structures of $\text{Arg}\cdot\text{Ba}^{2+}$ (**E** and **F**). Structure **NT**O of $[\text{Val} - \text{H} + \text{Ba}]^+$, in which the metal ion is solvated by the N-terminal amino group

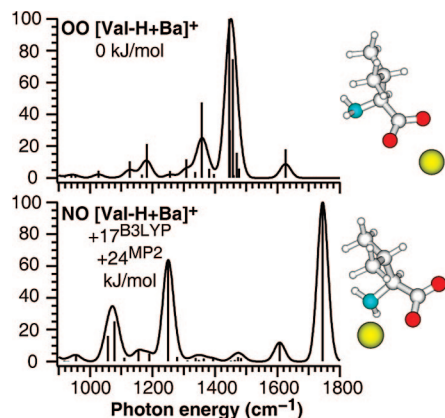


Figure 9. Calculated absorbance spectra for two low-energy structures of $[\text{Val} - \text{H} + \text{Ba}]^{2+}$. Relative B3LYP/6-311++G(2d,2p)//6-31+G(d,p) and MP2/6-311++G(2d,2p)//B3LYP/6-31+G(d,p) free energies at 298 K are reported for each conformer.

and one oxygen atom of the carboxylate group, is likely a good analogue for structures **G** and **I** of $\text{Arg} \cdot \text{Ba}^{2+}$. The symmetric and asymmetric stretches of the carboxylate group are calculated to occur at 1308 and 1724 cm^{-1} , respectively. The former is very similar to those calculated for structures **G** and **I** of $\text{Arg} \cdot \text{Ba}^{2+}$, whereas the latter is moderately blue-shifted from those calculated for structures **G** and **I** of $\text{Arg} \cdot \text{Ba}^{2+}$, but much closer in frequency than those observed for the other amino acids complexed with barium. These results indicate that the carboxylate stretch frequencies are very sensitive to the site of metal coordination and the identity and charge of other functional groups in the ion.

The band centered near 1650 cm^{-1} , which also has a width of greater than 100 cm^{-1} for both spectra, is attributable to the NH bending modes of a guanidinium group. The most intense NH bending modes for structure **E** correspond to those of the two $\text{N}^{\text{H}}\text{H}_2$ groups (1624 and 1657 cm^{-1}) and that of the bonded $\text{N}^{\text{H}}\text{H}$ group (1668 cm^{-1}), whereas those for structure **F** correspond to the free $\text{N}^{\text{H}}\text{H}$ group (1612 cm^{-1}), the free $\text{N}^{\text{H}}\text{H}_2$ group (1633 cm^{-1}), and the bonded $\text{N}^{\text{H}}\text{H}_2$ group (1691 cm^{-1}). Note that the most intense IRMPD band of protonated arginine, which also adopts a structure with a protonated side chain, is centered near 1670 cm^{-1} , is also quite broad, and is assigned to NH bending modes.¹⁴

Effect of Metal Ion Size on Zwitterion Stability. Calculations indicate that the zwitterionic form of arginine becomes progressively more stable with increasing alkaline earth metal size, consistent with these experiments that indicate that arginine adopts a zwitterionic form when complexed with divalent strontium or barium. It was recently reported that metal ion binding energies are better correlated to relative zwitterionic stability than metal ion size for alkali, alkaline earth, and transition metal cationized tryptophan.³⁷ We find this not to be the case for arginine complexed with divalent alkaline earth metal ions. Metal ion binding energies at 298 K were calculated at the B3LYP/6-311++G(2d,2p)//6-31+G(d,p) level of theory for each structure of $\text{Arg} \cdot \text{M}^{2+}$. The energy for isolated arginine was determined by evaluating several low-energy structures reported by Ling et al.⁶³ and structure “c4” was lowest in free energy at this level of theory.

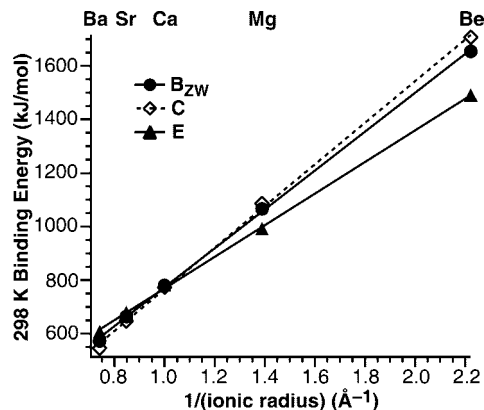


Figure 10. B3LYP/6-311++G(2d,2p)//6-31+G(d,p) calculated binding energies at 298 K versus inverse ionic radii.⁶⁴

Table 1. Linear Regression Statistics for Binding Energies versus Inverse Ionic Radius

| structure | slope ($\text{\AA} \text{ kJ mol}^{-1}$) | intercept (kJ mol^{-1}) | R^2 |
|-----------------------|--------------------------------------------|------------------------------------|--------|
| A | 769 ± 9 | -10 ± 12 | 0.9996 |
| B_{NZ} | 736 ± 4 | -14 ± 5 | 0.9999 |
| C | 778 ± 14 | -12 ± 18 | 0.9991 |
| B_{ZW} | 725 ± 9 | 48 ± 12 | 0.9995 |
| E | 590 ± 8 | 179 ± 11 | 0.9994 |
| F | 592 ± 8 | 179 ± 10 | 0.9995 |
| G | 669 ± 12 | 86 ± 17 | 0.9990 |
| I | 675 ± 11 | 75 ± 15 | 0.9991 |

For a given conformer of cationized arginine, the B3LYP/6-311++G(2d,2p)//6-31+G(d,p) binding energy for a given alkaline earth metal is found to be inversely proportional to literature values for ionic radius;⁶⁴ these data for structures **B_{ZW}**, **C**, and **E** are shown in Figure 10. Linear regression statistics for all eight structures are shown in Table 1 and all R^2 correlation coefficients are ≥ 0.999 . This relationship suggests that, for a given structure, alkaline earth metal ion size primarily affects electrostatic interactions between the amino acid and the divalent metal ion. For comparison, plotting the binding energies versus the square of the inverse radius, suggestive of charge dipole interactions, yields R^2 correlation coefficients ranging from 0.975 to 0.990.

Although the binding energy to each structure is inversely proportional to ionic radius, each class of structures designated in Figure 6 has a characteristic slope and intercept. Differences in these values account for the change in structures from nonzwitterion to zwitterion with increasing alkaline earth metal ion size. The beryllium and magnesium binding energies are greatest for structure **C**, whereas calcium, strontium, and barium binding energies are greatest for structure **E** (Figure 10). Relating the differences in regression statistics to other physical quantities is a topic of ongoing research and will likely provide additional insights into the effects of metal ion coordination on biomolecular structure.

General Comments on Level of Theory. A variety of basis sets and effective core potentials (ECP) were evaluated to determine their effect on the calculated spectra of amino acids complexed with barium. The most important factor was the ECP. The LANL2DZ ECP has 3s and 3p valence shell basis functions for Ba.⁶⁵ Frequencies for the carboxylate asymmetric stretch for the aliphatic amino acids calculated with this ECP are ~ 50

(63) Ling, S. L.; Yu, W. B.; Huang, Z. J.; Lin, Z. J.; Haranczyk, M.; Gutowski, M. *J. Phys. Chem. A* **2006**, *110*, 12282–12291.

(64) Shannon, R. D. *Acta Crystallogr. A* **1976**, *32*, 751–767.

(65) Hay, P. J.; Wadt, W. R. *J. Chem. Phys.* **1985**, *82*, 299–310.

cm^{-1} blue-shifted relative to the corresponding bands in the IRMPD spectra when scaling factors that yield good fits to the remaining bands are used. In contrast, good agreement was achieved for ECPs that include d shells, namely, the CRENBL ECP (5s,5p,4d valence)⁵⁹ and SRSC-f, an ECP in which the f valence shell is removed from the 3s,3p,2d,1f SRSC ECP.⁵⁸ This indicates that d shell basis functions are important for accurately calculating vibrational spectra of amino acids complexed with Ba. Vibrational spectra calculated using the 6-31+G(d,p) and 6-31++G(d,p) basis sets on all remaining atoms yielded nearly identical vibrational spectra, whereas spectra calculated using the 6-311+G(d,p) basis set on all remaining atoms yielded slightly poorer fits to the experimental data. In general, a 0.975 scaling factor yielded the best match for calculations with both the 6-31+G(d,p) and 6-31++G(d,p) basis sets (excluding the carbonyl stretch when the LANL2DZ ECP is used for Ba). For comparison, many studies have reported scaling factors of 0.975 or 0.98 when comparing B3LYP harmonic frequencies calculated using these basis sets with IRMPD spectra of cationized amino acids and peptides.^{14,15,38} On the basis of these results, the SRSC ECP was used for Sr, the CRENBL ECP was used for Ba, the 6-31+G(d,p) basis set was used for all remaining atoms, and vibrational frequencies were scaled by 0.975.

Note that there are attendant uncertainties in comparing absorbance spectra calculated at 0 K using the double-harmonic approximation with experimental action spectra obtained at finite temperatures. These effects contribute to differences between the experimental spectra and those calculated. However, the vast majority of the IRMD bands can be assigned to modes for low-energy candidate structures calculated with these uncertainties, and the assignments are consistent with those made for other amino acids complexed with monovalent or divalent metal ions.

Conclusions

The IRMPD spectra of $\text{Pro}\cdot\text{Ba}^{2+}$ and $\text{Val}\cdot\text{Ba}^{2+}$ indicate that these amino acids adopt zwitterionic structures when complexed with barium. Although the proton affinities of Val and Pro are both relatively high for aliphatic amino acids, which has been shown to result in the preferential stabilization of the zwitterionic forms of alkali metal cationized aliphatic amino acids,^{16,66} the relative energies of the **OO**–**ZW** and **NO**–**NZ** structures of $\text{Val}\cdot\text{Ba}^{2+}$ are similar to those calculated for glycine, the amino acid with the lowest proton affinity,⁶⁷ complexed with barium.¹⁸ Therefore, we predict that all aliphatic amino acids will adopt zwitterionic structures when complexed with barium.

The IRMPD spectrum of $\text{Ser}\cdot\text{Ba}^{2+}$ provides compelling evidence that serine adopts a zwitterionic structure in this ion. Calculations indicate that the zwitterionic form of this amino acid is 1 and 2 kJ/mol lower in free energy than the nonzwitterionic form at the B3LYP/6-311++G(2d,2p)//6-31+G(d,p) and MP2/6-311++G(2d,2p)//B3LYP/6-31+G(d,p) levels of theory, respectively. This energy difference, which is significantly smaller than those calculated for $\text{Pro}\cdot\text{Ba}^{2+}$ and $\text{Val}\cdot\text{Ba}^{2+}$, is primarily attributable to the hydroxyl side chain of serine

that can solvate the metal ion in the nonzwitterionic form but is too short to solvate the metal ion in the zwitterionic form. These results, coupled with previously reported trends with metal ion size for alkaline earth metal cationized glycine^{18,19} and alkali metal cationized arginine^{10,13,14} and lysine,¹⁵ suggest that serine may adopt a nonzwitterionic structure when complexed with only a somewhat smaller alkaline earth metal ion. Therefore, $\text{Ser}\cdot\text{M}^{2+}$ is a particularly promising candidate for studying the effects of alkaline earth metal ion size on amino acid zwitterion stability. Additionally, these results suggest that the nonzwitterionic form of $\text{Thr}\cdot\text{Ba}^{2+}$ may be lowest in energy because the secondary alcohol in the Thr side chain may preferentially stabilize the nonzwitterionic form relative to the zwitterionic form as compared to $\text{Ser}\cdot\text{Ba}^{2+}$, the side chain of which contains a primary alcohol. For comparison, $\text{Thr}\cdot\text{Na}^+$ and $\text{Ser}\cdot\text{Na}^+$ adopt similar structures in which the metal ions are solvated by the hydroxyl oxygen of the side chain and additional function groups,^{43,44} but the sodium binding energy of Thr is about 5 kJ/mol greater than that of Ser.⁶⁸

The IRMPD spectrum of $\text{Gln}\cdot\text{Ba}^{2+}$ indicates that this amino acid adopts a zwitterionic structure in which divalent barium is solvated by both oxygen atoms of the carboxylate group and the amide side chain. This result is consistent with calculations, which indicate that the nonzwitterionic form is 2 and 14 kJ/mol higher in free energy at the B3LYP/6-311++G(2d,2p)//6-31+G(d,p) and MP2/6-311++G(2d,2p)//B3LYP/6-31+G(d,p) levels of theory, respectively. The IRMPD spectra of $\text{Arg}\cdot\text{Sr}^{2+}$ and $\text{Arg}\cdot\text{Ba}^{2+}$ are similar and are most consistent with structures in which the divalent metal ions coordinate to both oxygen atoms of the carboxylate groups of zwitterionic arginine and that the guanidinium group interacts with the N-terminal amino group. These structures are similar to those reported previously for arginine complexed with larger alkali metal ions^{10,13,14} but lack any interactions between the guanidinium and carboxylate groups. Experimental results for $\text{Arg}\cdot\text{Ba}^{2+}$ are consistent with calculations at both the B3LYP/6-311++G(2d,2p)//6-31+G(d,p) and MP2/6-311++G(2d,2p)//B3LYP/6-31+G(d,p) levels of theory. Experimental results for $\text{Arg}\cdot\text{Sr}^{2+}$ are consistent with B3LYP/6-311++G(2d,2p)//6-31+G(d,p) calculations, but MP2/6-311++G(2d,2p)//B3LYP/6-31+G(d,p) calculations indicate that alternative nonzwitterionic and zwitterionic structures are slightly lower in free energy.

Acknowledgment. All IRMPD spectra were measured at the FOM Institute for Plasma Physics “Rijnhuizen”, which is financially supported by the Nederlandse Organisatie voor Wetenschappelijk Onderzoek (NWO). We acknowledge Dr. B. Redlich and the FELIX staff for excellent support. Generous financial support was provided by National Science Foundations Grants CHE-0718790 (E.R.W.), CHE-0404571 (R.J.S.), and CHE-9909502 (travel support).

Supporting Information Available: Cartesian coordinates for all structures, full citation for ref 60, Supporting Information Figures 1 and 2, and Supporting Information Table 1. This material is available free of charge via the Internet at <http://pubs.acs.org>.

JA711343Q

(66) Lemoff, A. S.; Bush, M. F.; Williams, E. R. *J. Am. Chem. Soc.* **2003**, *125*, 13576–13584.

(67) Bleiholder, C.; Suhai, S.; Paizs, B. *J. Am. Soc. Mass Spectrom.* **2006**, *17*, 1275–1281.

(68) Kish, M. M.; Ohanessian, G.; Wesdemiotis, C. *Int. J. Mass Spectrom.* **2003**, *227*, 509–524.